Dynamic Interaction of Heavy Duty Vehicles and Expansion Joints

Daniel Rill[1]([✉]), Christiane Butz[1], and Georg Rill[2]

[1] Maurer Engineering GmbH, Frankfurter Ring 193, 80807 München, Germany
{d.rill,c.butz}@maurer.eu
[2] OTH Regensburg, Galgenbergstr. 30, 93053 Regensburg, Germany
georg.rill@oth-regensburg.de

Abstract. The "Smart Bridge (Intelligente Brücke)" project cluster, initiated by the German Federal Highway Research Institute (Bundesanstalt für Straßenwesen, BASt) and the Federal Ministry of Transport and Digital Infrastructure (BMVI), focuses on "smart" monitoring devices that allow an efficient and economic maintenance management of bridge infrastructures. Among the participating projects, the one presented herein focuses on the development of a smart expansion joint, to assess the traffic parameters on site. This is achieved by measuring velocity and weight of crossing vehicles. In reference measurements, performed with a three-axle truck and a typical tractor semi-trailer combination with five axles in total, it was shown that the interaction between the vehicle and the expansion joint is highly dynamic and depends on several factors. To get more insight into this dynamic problem, a virtual test rig was set up. Although nearly all vehicle parameters had to be estimated, the simulation results conform very well with the measurements and are robust to vehicle parameter variations. In addition, they indicate a significant influence of the expansion joint dynamic to the peak values of the measured wheel loads, in particular on higher driving velocities. By compensating the relevant dynamic effects in the measurements, a "smart" data processing algorithm makes it possible to determine the actual vehicle weights in random traffic with reliability and appropriate accuracy.

1   Introduction

The bridge equipped with important aspects of the "Smart Bridge" is part of the greater program "Digital Test Bed Motorway", which encompasses numerous projects under the common motto "Mobility 4.0" and stretches along the A9 between Nuremberg and Munich.

The structure (BW402e), built in 2015 at the motorway interchange Nuremberg, includes various sensor-equipped components, which are developed and investigated in several projects by a consortium. One aim is to better understand the correlation between bridge condition and traffic effects, in order to develop more accurate models for condition prognosis.

Among these components, one of the expansion joints of the bridge (located between the bridge deck and eastern abutment) was outfitted with sensors.

To gather calibration data, reference runs with two different trucks with defined weight and several velocity settings were conducted. Based on these data sets, an evaluation software was created, which continuously gathers and assesses the data to determine the traffic characteristics.

2   Measurement Setup

The smart expansion joint (installed and maintained by Maurer Group) was specially developed, based on a standard modular Swivel-Joist-Joint. While maintaining basic requirements, such as watertightness and conformity to building codes (by singular assessment according to TL/TP FÜ(2005)), the "smart" joint has some modifications to facilitate the intended measurements [1]. Mainly, the lamellae are physically separated between the lanes, so traffic can be evaluated for both lanes independently. The joint is also equipped with diamond shaped plates on top of the lamellae, which in this case serve a dual purpose: First, as in standard devices, they provide a reduction of the tire contact noise and second, they allow for a smoother force progression during each crossing event. The left image in Fig. 1 shows the working principle of the "smart" joint. Integrated into the control and support mechanism are sliding bearings with integrated load sensors. These measure the vertical loads on both ends of each support bar. Also, the first and third lamellae of each segment are connected to draw-wire sensors, which measure the current total gap width. This setup allows not only for a measurement of the total force which acts on the joint, but by comparing the load peaks on the front and rear side with the joint opening, the velocity of the vehicles can be calculated.
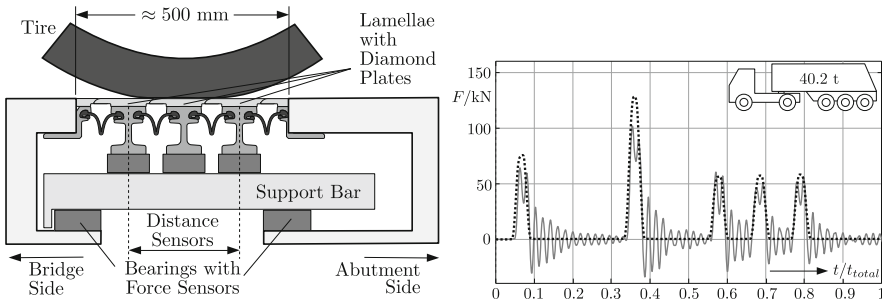

Fig. 1. Schematic longitudinal section of smart expansion joint with sensor locations and deviations between measurement at 90 km/h (solid line) and 5 km/h (dotted line)

From the data obtained by reference runs, it became apparent that the relation between static and (dynamic) measured load is dependent on the vehicle's velocity, cf. right plot in Fig. 1.

3 Virtual Test Rig

Appropriate models are required to describe the dynamic interaction between heavy duty vehicles and expansion joints.

For decades the multibody system approach has been successfully applied to all kind of vehicles, [2]. Complex vehicle models which may be set up by commercial multibody software packages or by appropriate modeling approaches will produce accurate simulation results only if a reliable set of parameters is available. In this particular case, however, just the wheel bases and the total mass of the test vehicles measured by the static axle loads were known. That is why rather simple two-dimensional models, like the planar model presented in [3] that describes the vertical dynamics of an agricultural tractor, were used to simulate the three-axle truck and the tractor semi-trailer combination, respectively. It turned out that the compliance of the expansion gap plays an important rule in the interaction between the vehicle and the expansion joint. A lumped mass approach to the expansion joint that takes relevant body deformations into account results in a comparatively lean three-dimensional model matching the accuracy of the vehicle models and providing an excellent run time performance.
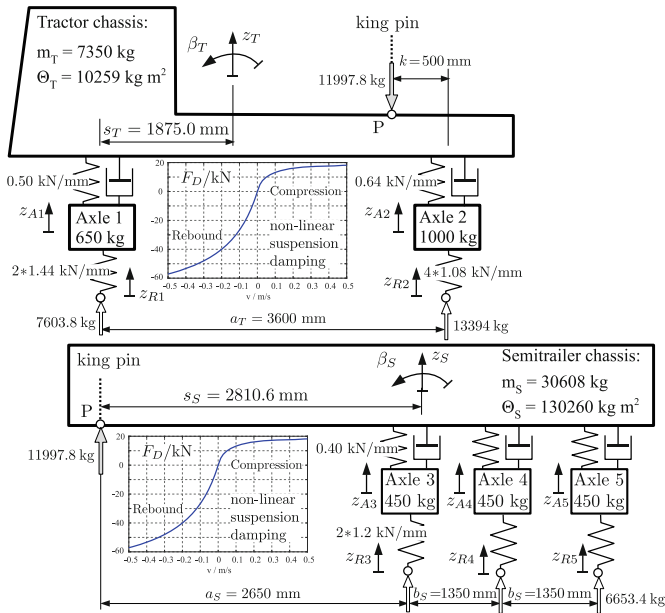
Fig. 2. Two-dimensional model of a tractor/semitrailer combination with model parameters

The two-dimensional model for the tractor/semi-trailer combination is separated into two parts, cf. Fig. 2. The first model has $f_T = 4$ degrees of freedom

that are represented by the tractor chassis hub motion z_T, the tractor chassis pitch motion β_T, and the vertical displacements of the front z_{A1} and the rear z_{A2} axles. A three-axled truck is then modeled simply by adding a second rear axle with the corresponding vertical axle displacement z_{A3} as an additional degree of freedom. The second model represents the semitrailer that has no front axle but three rear axles. It has $f_S = 5$ degrees of freedom represented by the semitrailer chassis hub motion z_S, the semitrailer chassis pitch motion β_S, and the vertical displacements z_{A3}, z_{A4}, z_{A5} of the three rear axles. The two vehicle parts are coupled by a constraint equation provided by the revolute joint located at point P on the king pin line that approximates the real 5th-wheel coupling in this two-dimensional approach. Only the wheel bases and the static axle loads are known. The derived and estimated parameters of the tractor and the semi-trailer are provided in Fig. 2. Here, also the mass of the unloaded truck had to be esti-mated in order to derive the mass of the trailer and the load at the kingpin. The pneumatic coupling between the three rear axles of the trailer is neglected because it will act rather slowly and hence will not influence a rather fast expan-sion joint crossing maneuver. The equations of motion for the tractor and the semi-trailer result in two coupled sets of second order differential equations

$$\mathbf{M}_T\,\mathbf{y}_T = \mathbf{q}_T + \lambda \left(\frac{dg}{d\mathbf{y}_T} \right)^T \quad \text{and} \quad \mathbf{M}_S\,\mathbf{y}_S = \mathbf{q}_S + \lambda \left(\frac{dg}{d\mathbf{y}_S} \right)^T \quad \text{as well as}$$
$$g = g(\mathbf{y}_T, \mathbf{y}_S) = z_T + (a_T - s_T - k)\,\beta_T - (z_S - s_S\,\beta_S) = 0 \tag{1}$$

that represent a system of differential algebraic equations (DAEs) in an index 3 notation, where $\mathbf{M}_T$ and $\mathbf{M}_S$ are the corresponding mass matrices, the vectors $\mathbf{q}_T$ and $\mathbf{q}_S$ represent the generalized forces and torques applied to the tractor and the semitrailer, the vectors $\mathbf{y}_T$ and $\mathbf{y}_S$ collect the generalized coordinates of each vehicle part. Small pitch angles $\beta_T \ll 1$ and $\beta_S \ll 1$ can be taken for granted here which simplifies the constraint equation $g(\mathbf{y}_T, \mathbf{y}_S) = 0$ and its derivatives $dg/d\mathbf{y}_T$ and $dg/d\mathbf{y}_S$. The Lagrange multiplier λ automatically provides appropri-ate coupling forces to the tractor and the semitrailer, [4]. DAE systems of index 3 can be solved by index-reduction where the constraint equation is transferred from the position to the acceleration level. Finally, an approriate Baumgarte stabilization is applied to avoid a drift in the constraint equation, [5]. The cho-sen stabilization eigenfrequency of $f_C = 10$ Hertz and a viscous damping rate of $\zeta_C = 0.5$ will avoid too high frequencies in the stabilization but still grant a sufficient fast and smooth decay of any deviations in the constraint equation. The vectors of generalized forces and torques incorporate the suspension forces

$$F_{Si} = c_{Si}\,u_i + F_D\,(v_i) \quad \text{with} \quad F_D\,(v_i) \;=\; \begin{cases} d_0\,\frac{v_i}{1+p_C v_i} & \text{if } v_i \geq 0 \\ d_0\,\frac{v_i}{1-p_R v_i} & \text{if } v_i < 0 \end{cases} \tag{2}$$
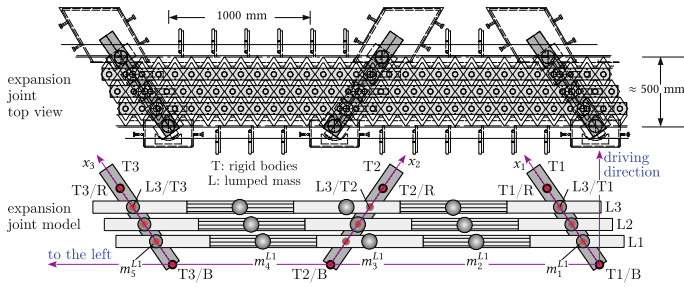
Fig. 3. Top view of one part of the expansion joint and corresponding lumped mass model

where the parameter c_{Si} denotes the stiffness of the corresponding suspension springs and d_0 the overall suspension damping constant at $v_i = 0$. The parameters $p_C > 0$ and $p_R > p_C$ generate a degressive damping characteristic that differs in compression and rebound mode. Although the suspension stiffness is modeled differently at the front and the rear axles, the same damping parameters were applied at each axle as typical for the layout of heavy duty trucks. The static and dynamic axle loads are provided by

$$F_{Ti}^S = \hat{c}_{Ti}\left(z_{Ri} - z_{Ai}\right) \quad \text{and} \quad T_D\,\frac{dF_{Ti}^D}{dt} = F_{Ti}^S - F_{Ti}^D \quad \text{or} \quad \frac{dF_{Ti}^D}{dt} = \frac{1}{T_D}\left(F_{Ti}^S - F_{Ti}^D\right) \tag{3}$$

where $\hat{c}_{Ti}$ denotes the overall tire stiffness at each axle, z_{Ri} is the average height of the road or expansion joint respectively and z_{Ai} describes the vertical displacement of the axle. The dynamic loads F_{Ti}^D generated by the first order differential equations are distributed equally to each tire, hence representing the load that is applied to the road or the expansion joint respectively.

The expansion joint, as depicted in Figs. 1 and 3 is modeled by a lumped mass system where each lamella (L1, L2, L3) was approximated by five modal masses (m_1^{L1} ... m_5^{L3}) in order to model the bending eigenmodes. A 4th-order polynomial defined by the vertical displacements of the 5 point masses provides the deflection of each lamella at arbitrary points. The support-bars or traverses (T1, T2, T3) were described by rigid bodies with hub and pitch about their local lateral axis (y_1, y_2, y_3) as degrees of freedom. Small pitch angles can be taken for granted here. The rubber mounts that connect the lamellae with the support-bars (T1/L1, ... T3/L3) and the traverses with the bridge (T1/B, T2/B, T3/B) or the road (T1/R, T2/R, T3/R), respectively, were modeled by simple linear spring damper combinations. Hence, the multibody model of the expansion joint is linear and has in total $f = 3*5 + 3*2 = 21$ degrees of freedom that reproduce eigenmodes of the vertical vibrations in the range from 98 to 986 Hz.
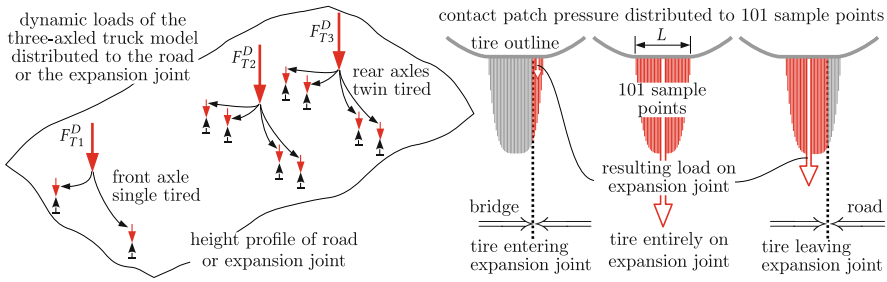
**Fig. 4.** Interaction between vehicle (three-axled truck) and expansion joint

To couple the two-dimensional vehicle models with the three-dimensional expansion joint model, the dynamic wheel loads, in case of the three-axle truck F_{T1}^D to F_{T3}^D, are equally split into corresponding wheel loads according to the number of tires mounted to each axle, left image in Fig. 4. The wheel or tire loads are distributed over the contact patch. Within the two-dimensional vehicle models, just the load distribution into the longitudinal direction is taken into account. According to [6] the length of the contact patch depends on the wheel load and the unloaded tire radius.

By using the dynamic axle load, this length can be calculated prior to the contact calculation itself.

The contact length L determines the distribution of the load between the bridge deck, expansion joint and the road surface, right image in Fig. 4. To distribute the dynamic tire loads properly, the contact patch was discretized by 101 sample points and the pressure distribution along the contact length was assumed to follow a 4th-order polynominal.

4 Simulation Results

As seen in Fig. 5, the measured forces represented by the peak-values correspond accurately with the steady state axle loads (F_1^0 to F_5^0) of the two test vehicles at low velocities ($v \approx 30$ km/h). With increasing driving velocity v, the time history of the resulting force $F = F(t)$ becomes more and more dynamic. On this particular expansion joint the first bending eigen-mode of the lamellae occurs at a frequency of $f \approx 100$ Hz and generates a double peak and a significant transient response that causes fluctuations in the time history of the measured signal even when the axle has passed the expansion joint. The simulation provides the movements of the vehicles too. In all runs, the pitch motions were limited to a few angle seconds which indicates that the most uncertain inertia properties of the truck, tractor, or semitrailer chassis will have no impact on the results. A reduced suspension damping results in quite different chassis and axle movements, but the influence on the forces exposed to the expansion joint is not noticeable.
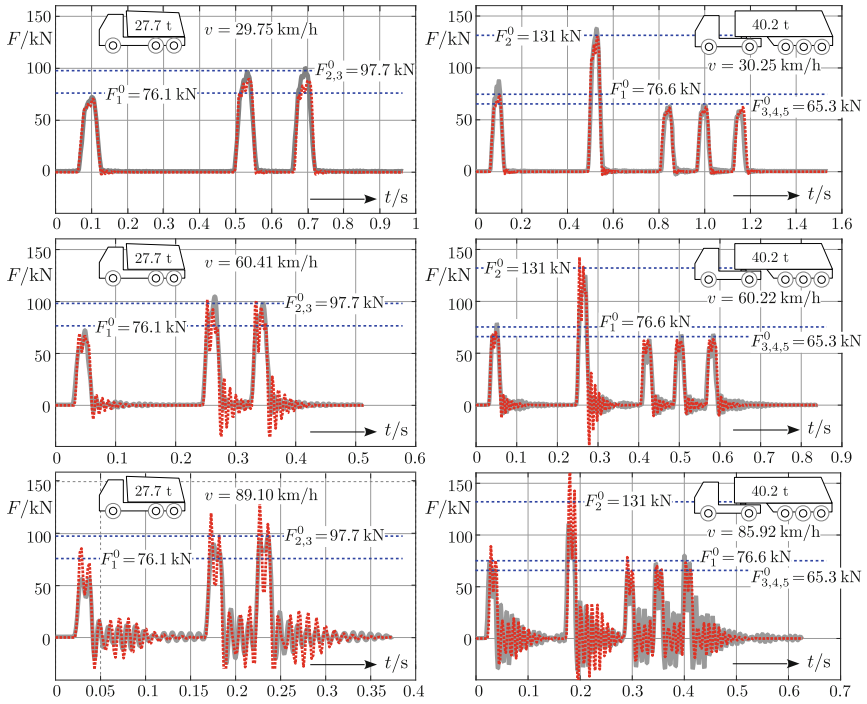
Fig. 5. Comparison between measurements (solid gray) and simulation results (dotted red) at different driving velocities where the dotted blue horizontal lines mark the static axle loads

5   Data Processing

With the insights gained from the virtual experiments, a correction algorithm could be developed, which allows for a compensation of the dynamic influence. As it was found that mainly the vibrations of the joint are responsible for the
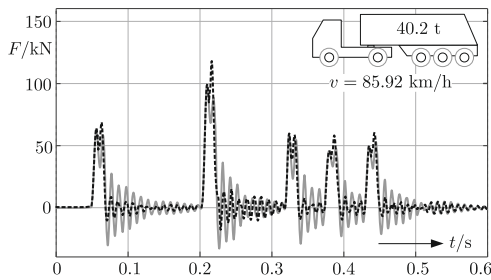
Fig. 6. Smart correction of measured signal. The solid gray line represents the raw measured signal. The dotted black line shows how the compensation algorithm has closely reconstructed the quasi-static values by subtracting the dynamic contribution.

measurement errors, the dynamic contribution to the force signal can be isolated and compensated for. Presently, the dominant eigenfrequency of the joint is modeled to be excited by the initial tire contact. The known progression of this oscillation can then be used to reconstruct the quasi-static load from the measured signal, as shown in Fig. 6.

6   Conclusion

The planar vehicle models combined with the 3-dimensional lumped mass model of the expansion joint are able to reproduce the dynamics of the joint crossing very well. In a wide range, the results are not sensitive to internal vehicle parameters. Hence, the measured loads will reproduce the axle loads very accurately. At higher velocities, the dynamics of the expansion joint and its height profile influence the results. But, it is possible to compensate for these effects because the parameters of the expansion joint are well known or can be identified with sufficient accuracy. The simulation results showed that the lateral offset of a vehicle is also important. By analyzing the measurements this offset can be calculated too. The simple estimation applied here already results in a significant improvement. Knowing the impact of the vehicle and joint parameters has allowed the development of a robust and fast correction algorithm which improves the quality of the measured traffic load.

References

1. Butz, C., Rill, D.: Smart expansion joints and smart bearings embedded in the "Intelligente Brücke im Digitalen Testfeld Autobahn" (Intelligent Bridge of the Digital Motorway Test Bed). In: Proceedings of the 12th - Japanese-German Bridge Symposium, Munich, Germany, 4.9.-7.9 (2018)
2. Gipser, M., Rill, G.: Simulation komplexer Fahrzeugsysteme und Ergebnisdarstellung in rechnererzeugten Filmen, in Dynamik gekoppelter Systeme, VDI-Bericht, vol. 603. VDI-Verlag (1986)
3. Rill, G., Schaeffer, T.: Grundlagen und Methodik der Mehrkörpersimulation, 3rd edn. Vieweg, Wiesbaden (2017)
4. Rill, G., Chucholowski, C.: Real time simulation of large vehicle systems. In: ECCOMAS Multibody Dynamics, Milano, Italy (2007)
5. Rill, G.: Multibody systems and simulation techniques. In: Lugner, P. (ed.) Vehicle Dynamics of Modern Passenger Cars, pp. 309–375. Springer International Publishing (2019)
6. Rill, G.: Road Vehicle Dynamics. Taylor & Francis, Boca Raton (2012)